RESEARCH ARTICLE

On the phenology and seeding potential of sea-ice microalgal species

Maria A. van Leeuwe[1,*], Mairi Fenton[2], Emily Davey[3], Janne-Markus Rintala[4], Elizabeth M. Jones[5], Michael P. Meredith[6], and Jacqueline Stefels[1]

Sea ice is an important habitat for a wide variety of microalgal species. Depending on the species composition, sea ice can be a seeding source for pelagic phytoplankton blooms after ice melt in spring. Sea-ice algal communities were studied over 2 full winter seasons in 2014 and 2016 at Rothera Research Station, situated at the Western Antarctic Peninsula (WAP). Algal pigment patterns and microscopic observations were combined with photophysiological studies based on fluorescence analyses to monitor and explain the phenology of ice-algal species. Clear patterns in species succession were identified. Young sea ice contained a mixture of algal species including dinoflagellates, cryptophytes and diatoms like *Chaetoceros* spp. and *Fragillariopsis* spp. In winter, severe environmental conditions resulted in a decline in species diversity and selection towards heterotrophy. Pennate diatoms like *Amphiprora kufferathii* and *Berkeleya adeliensis* were the first to dominate the nutrient-enriched bottom-ice layers in early spring. The bottom communities exhibited a remarkably stable value for the photoadaptation parameter, E_k, of circa 25 μmol photons m^{-2} s^{-1}. Whereas pennate diatoms were most abundant in spring ice, the initial seeding event linked to ice melt was associated with flagellate species. Haptophyte species like *Phaeocystis antarctica* and prymnesiophytes like *Pyramimonas* spp. best sustained the transition from sea ice to seawater. Comparison with previous studies shows that the seeding patterns observed in Ryder Bay were characteristic over the wider sea-ice domain, Arctic and Antarctic. Over the course of this century, the WAP is predicted to experience continuing thinning and decline in sea-ice cover. For the near future, we expect that especially microalgal communities of haptophytes and chlorophytes will benefit from the changes, with yet unknown implications for carbon fluxes and higher trophic levels.

Keywords: Biogeochemistry, Haptophytes, Phenology, Pigments, Sea ice, Seeding

1. Introduction

Sea ice covers more than 10% of the world's oceans and forms a unique habitat in polar regions. In spring and summer, the ice is very rich in algal biomass and supports a wealth of organisms, such as seals and penguins (Thomas, 2017, and references therein). Primary production in sea ice can be very high and may locally represent 2–24% of oceanic primary production (Legendre et al., 1992; McMinn et al., 2010; Arrigo, 2014). Especially in bottom-ice layers, large algal biomass may accumulate, which forms an important food source for organisms dwelling in and under the ice pack (Meiners et al., 2018). In winter, bottom-ice algae are the main food source for higher trophic levels and key Antarctic species like krill (Thomas, 2017).

Sea-ice algal communities are important not only for the marine ecosystem, but also because they play a key role in climate regulation. Sympagic (sea-ice associated) microalgae may shuttle significant amounts of carbon from the atmosphere into sea ice and from there into the oceans. In spring, the rapid release of microalgae from the melting sea ice may result in carbon fluxes, away from the euphotic zone, of 5–10 mg C m^{-2} d^{-1} (Buesseler et al., 2003). Sea ice is also a potential source for the climate-active gas dimethylsulphide (DMS), a breakdown product of dimethylsulphoniopropionate (DMSP). When released into the atmosphere DMS plays an important role in cloud formation and thus a pivotal role in climate regulation (Stefels et al., 2007). Whereas all algal growth depends on CO_2 uptake, DMSP production is limited to specific algal species and dependent on environmental conditions

[1] The Groningen Institute of Evolutionary Life Sciences (GELifeS), University of Groningen (RUG), Groningen, the Netherlands
[2] Heriot-Watt University, Edinburgh Campus, Edinburgh, UK
[3] Bermuda Institute of Ocean Sciences, St. George's, Bermuda
[4] INAR—Institute for Atmospheric and Earth System Research, Faculty of Agriculture and Forestry, University of Helsinki, Helsinki, Finland
[5] Institute of Marine Research, Fram Centre, Tromsø, Norway
[6] British Antarctic Survey, Cambridge, UK

* Corresponding author:
Email: m.a.van.leeuwe@rug.nl

(Stefels et al., 2007). Particularly in sea-ice dominated areas, biological production of DMSP can be the major source of atmospheric DMS (Galindo et al., 2014; Stefels et al., 2018).

The sea-ice environment is highly dynamic in space and time and governed by the annual solar cycle. The changing conditions in light, temperature and ice formation exert strong influence on the composition and concentration of resident algal communities, with ensuing succession of algal species (Leu et al., 2015; Arrigo 2017; Van Leeuwe et al., 2018). In autumn, a mixed algal community is incorporated in the growing ice body, by passive aggregation to newly formed ice particles, as well as through migration of the ambient pelagic community into the relatively sheltered pockets of the sea ice (Garrison et al., 2005). Extreme conditions in winter select for a limited number of species, leaving mainly pennate diatoms and mixotrophic flagellates (Rozanska et al., 2009). Spring is characterized by a succession of diatom and algal groups, where the composition is influenced by environmental conditions of light and temperature (Leu et al., 2015).

The fate of the spring sympagic community is variable and poorly described. Rapidly changing conditions in melting ice may result in the release of deteriorating algal communities, which can form large aggregates that quickly sink out of the euphotic zone (Riebesell et al., 1991). Subsequently, this material will be exported to the deep ocean. The release of sympagic algae, however, may also elicit the onset of large phytoplankton blooms in the marginal ice zone (MIZ) (Smith and Nelson, 1990; Galindo et al., 2014), where nutrients are in ample supply and grazing pressure is relatively low (Lancelot et al., 1991; Arrigo, 2014). Although the relation between algal communities in sea ice and the pelagic environment has been explored in various studies (Garrison et al., 1987; Lizotte, 2001; Ratkova and Wassmann, 2005; Selz et al., 2018a; Selz et al., 2018b), a consistent seeding pattern has not yet been described, leaving the link between the sea-ice and pelagic ecosystems unclear.

The polar regions are amongst the most susceptible places on Earth to climate change, with major atmospheric warming of 3°C along the Western Antarctic Peninsula (WAP) during the second half of the twentieth century, coinciding with significant warming of coastal and surface waters (Meredith and King, 2005). These increases in seawater temperature have been accompanied by a decline in sea-ice cover and reduction in the sea-ice season of 85 days (Stammerjohn et al., 2008). In recent years, the trends have slowed and future predictions for the Southern Ocean are uncertain (Turner at al., 2016; Meredith et al., 2019). Yet, ongoing global warming will not leave the Southern Ocean unaffected (Henley et al., 2019), with consequences for microalgal communities in sea ice and in the ocean (Van Leeuwe et al., 2020).

The link between sea ice and the pelagic system depends on their respective community composition. The phenology of sea-ice microalgae has been outlined for algal classes, but details on species composition are still lacking. Therefore, predicting the impact of ongoing climate change on the linkages between the atmosphere-sea
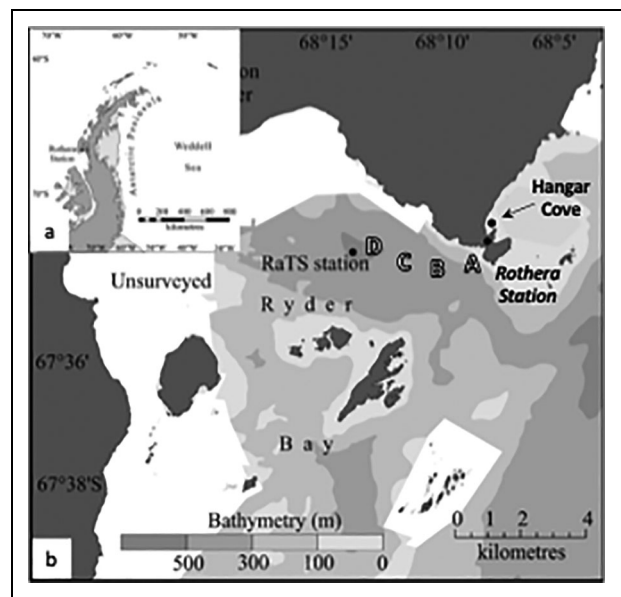
Figure 1. Map of the study area. (a) The location the British research station Rothera at the Western Antarctic Peninsula and (b) the locations of the ice stations at Hangar Cove (arrow) and along the transect (A–D), and the site of seawater sampling near the Rothera Time Series (RaTS) station located in Ryder Bay. DOI: https://doi.org/10.1525/elementa.2021.00029.f1

ice-ocean compartments is difficult (Tedesco et al., 2012). Here we present results from an extensive time-series study at Ryder Bay, during which microalgal communities in sea ice and the ocean were investigated. In a previous paper on microalgal phenology in the waters of Ryder Bay, we predicted that in the near future more extensive blooms could occur in the MIZ (Van Leeuwe et al., 2020). In this paper, we present the data collected in sea ice in Ryder Bay, studied over 2 full winter seasons in 2014 and 2016, complemented by brief sampling events in 2013 and 2015. Algal species composition and associated biogeochemical parameters were studied in detail. Sea-ice sampling was combined with water sampling to monitor the link between sea-ice algae and the ocean and generate improved understanding of the mechanisms that drive the annual patterns in the biogeochemistry of sea-ice ecosystems.

2. Material and methods
2.1. Sampling
2.1.1. Ice core sampling
Sea-ice cores were collected from newly formed land-fast sea ice in Hangar Cove (67.564°S, 68.130°W) at Rothera Research Station, West Antarctic Peninsula (**Figure 1**). In 2014 and 2016, two complete seasons were sampled, from ice formation in austral autumn until melt in spring–summer. Incidental cores were also collected in 2013 and 2015 (**Table 1**; see Table S1 for a complete overview). In winter, cores were collected every 2–4 weeks. In November and December, cores were taken more frequently. On September 30, 2014, four stations along a transect (A–D)

Table 1. Summary of the number of ice cores that were sampled for various parameters over the years. DOI: https://doi.org/10.1525/elementa.2021.00029.t1

Year	First–Last Coring Date	Pigments	POC[a]	^{13}C-Uptake	DIC[b]	PAM[c]	Nutrients	Cell Counts
2013	Aug 2–Sep 27	4	na[d]	na	na	5	na	na
2014	Aug 17–Dec 20	22	4	3[e]	8	16	17	14 (2[e])
2015	July 28–Oct 14	4	na	na	4	na	na	na
2016	Apr 22–Dec 9	22	22	3	na	15	18	2 (1[e])

[a] Particulate organic carbon.

[b] Dissolved inorganic carbon.

[c] Photosynthetic performance using a pulse-amplitude-modulated fluorometer.

[d] Not available.

[e] Under-ice samples collected by divers.

were sampled to examine the spatial heterogeneity of microalgae in the sea ice in Ryder Bay (**Figure 1**).

Cores were taken using a 0.09-m diameter ice corer (Kovacs). The ice area was predominantly free of snow, with isolated patches of snow cover, during spring and summer. Cores were immediately sliced in sections: the bottom section always measured 5 cm, followed by 10–15 cm sections towards the surface of the core. Sections were kept in the dark during transport to the laboratory. Cores were melted in hypersaline water, at 4°C, under dark conditions, over 24–40 h, to arrive at a final salinity between 25 and 35 (see Miller et al., 2015, for discussion on melting procedures). After melt, subsamples for algal pigments, particulate organic carbon (POC), fluorescence analyses, nutrients and cell counts were taken under dim light. A single ice core was taken per sampling event. In 2014 and 2015, an additional core was taken for carbonate chemistry (for full details, see Jones et al., 2022).

2.1.2. Seawater sampling

Under-ice seawater was collected during the transition of spring into summer using a 12 V electric bilge pump with silicon tubing, with the inlet lowered to the ice-water interface (0.10-m depth) (December 2014). In 2014 and 2016, samples from the sea-ice water interface were taken by divers using a 50-ml syringe. In addition, seawater samples were taken at the Rothera Time Series station at 67.570°S 68.225°W in Ryder Bay in 2014 and 2016 (**Figure 1**). These samples were collected at 5 and 15 m with a Niskin bottle and a hand winch from a small boat. Samples were stored in the dark and at ambient temperature for return to the laboratory, where subsamples were taken for algal pigments and cell counts. See Van Leeuwe et al. (2020) for oceanographical details and a full description of the pigment data in the pelagic realm between 2012 and 2017.

2.2. ^{13}C-uptake experiments

Photosynthesis rates were determined by ^{13}C-carbon incorporation into POC. Two types of experiments were performed. In 2014, experiments were performed with ice-associated communities collected by divers. In order to distinguish in-ice communities from long ice-associated strands, the samples were gently filtered over a 300-μm size mesh before incubation in polystyrene tissue-culture flasks. Photosynthesis-irradiance (P-I) relationships were established by incubations of duplicate samples for 8–10 h at 1, 10, 50 and 150 μmol photons m^{-2} s^{-1}. In 2016, P-I relationships were established for algal communities loosely attached to bottom ice at 5, 10, 18, 50, 120 and 150 μmol photons m^{-2} s^{-1}. In addition, ice-core samples were incubated at a standard light intensity of 65 μmol photons m^{-2} s^{-1} over 48 h to establish a vertical profile of the growth capacity. After sea-ice melt, 50-ml subsamples were transferred into culture flasks. Before incubation, all samples were enriched with NaH^{13}CO$_3$ (5–8% final solution). Incubations were terminated by filtering the samples over combusted GF/F Whatman filters and stored at −20°C until analyses at the University of Groningen. Values for specific carbon incorporation rate, μ_{POC} (h^{-1}), were derived from the equation for production in Stefels et al. (2009):

$$\mu_{POC}(h^{-1}) = \ln[(R_m - R_b)/(R_m - R_t)]/\partial t.$$

where R_m is the maximal ^{13}C/(^{12}C + ^{13}C) ratio measured in the total dissolved inorganic carbon (DIC), R_b is the ratio of ^{13}C/(^{12}C + ^{13}C) in POC at t_0, and R_t is the ratio in POC after incubation. Rate values obtained in the P-I experiments were taken to calculate the maximum growth capacity P^C_{max} and light affinity α^C (electrons quanta^{-1}), using a non-linear fit (Prism) based on the P-I equation of Platt et al. (1980). These values were used to calculate the index for photoadaptation, E_k, as P^C_{max}/α^C. Duplicate ^{13}C-uptake experiments were performed 3 and 2 times in December 2014 and 2016, respectively.

2.3. Analyses
2.3.1. Pigment analyses
A sample volume of 50–500 ml for ice samples and 1000–5000 ml for seawater was filtered gently (< 15 kPa) over a Whatman GF/F filter, subsequently snap-frozen in liquid nitrogen, and stored at −80°C until analysis at the

University of Groningen. Before extraction in 90% acetone, filters were freeze-dried at −55°C for 48 h. Pigments were analysed by high-performance liquid chromatography (HPLC) on a Waters system equipped with a photodiode array detector (Van Heukelem and Thomas, 2001; van Leeuwe et al., 2006). A Zorbax C8, 3.5-µm column was used. Pigment standards were obtained from DHI Water Quality Institute (Horsholm, Denmark). Chlorophyll *a* (Chl *a*) concentrations in bottom sea ice from October to December were used to calculate net community growth, applying an exponential fit: $\mu^{Chl\ a}$ (d^{-1}) (Microsoft Excel).

2.3.2. Carbon analyses
POC was analysed by cavity ring-down spectroscopy. A sample volume of 50-2000 mL was filtered gently (< 15 kPa) over a pre-combusted Whatman GF/F filter and stored at −20°C until analysis in the home laboratory. To remove inorganic carbon before analysis, filters were left in an exicator with 4 ml 37% fuming HCl for 4 h and dried at 60°C overnight. Samples were analysed with a combustion module attached to a cavity ring-down spectroscopy analyser, which distinguishes the isotopes ^{12}C and ^{13}C (CM-CRDS, with a G2101-i Analyzer, Picarro, California, USA). The $\delta^{13}C$-POC signature of in situ samples was analysed only for samples taken in 2014. The $\delta^{13}C$ stable isotope composition was calculated relative to the international Vienna Pee Dee Belemnite standard.

The $\delta^{13}C$-signature of total dissolved inorganic carbon samples that were taken for experimental purposes were analysed by purging the samples with the carrier gas nitrogen, after acidification with phosphoric acid and analysed with the Picarro.

DIC was analysed using a VINDTA 3C (Versatile INstrument for the Determination of Total Alkalinity, Marianda). Samples were extracted from a sibling ice core. Sections of 10 cm were packed in gas-tight Tedlar bags, evacuated and left to melt at 20°C without the addition of seawater. After melt, samples were acidified with 8.5% H_3PO_4, and DIC was analysed by coulometric analysis (Johnson et al., 1987). Samples were collected over 2 successive years but are presented as a pseudo-seasonal time series.

2.3.3. Chlorophyll fluorescence parameters
Photosynthetic performance was assessed using a pulse-amplitude-modulated (PAM) fluorometer (Water PAM, Heinz Walz, GmbH). Prior to each analysis, samples were dark-adapted for 10 min. In 2013 and 2014, sea-ice samples were concentrated after melt on a GF/F Whatman filter under mild (< 15 kPa) vacuum, preventing the filter from drying completely. The filters were placed on a moist tissue arranged on a cool plate inside a coolbox, for subsequent fluorescence analyses with fiber optics. Sea-ice samples collected in 2016 and all seawater samples were analysed using a cuvette. In 2014, the filtration method had been tested and compared to the classical 'cuvette-analyses', which did not result in significant differences. Rapid light curves were established by 30-s exposure to 0, 10, 40, 70, 110, 160, 220, 290, 350 and 400 µmol photons m^{-2} s^{-1}. The first recording of the light curves provides the maximum quantum yield of photosynthesis

(Fv/Fm). The maximum photosynthetic capacity, P$_{max}$, and light affinity, α (electrons quanta^{-1}), were determined using a non-linear fit (Prism) based on the P-I equation by Platt et al. (1980). In this paper only α is discussed. The results for P$_{max}$ were highly variable, most likely due to low biomass.

2.3.4. Nutrient analyses
Samples were filtered (0.2-µm discs, Whatman PLC, UK) and stored at −20°C (nitrate plus nitrite, phosphate) or 4°C (silicic acid) until analysis, using a Technicon TRAACS 800 Autoanalyzer (Bran and Luebbe GmbH) following standard methods (Grasshoff, 1983). Detection limits were 0.01, 0.02, and 0.26 µM for phosphate, nitrate plus nitrite, and silicic acid, respectively. For full details see Jones et al. (2022).

2.3.5. Cell counts
For the determination of cell numbers and species composition, 5-ml samples were collected after ice melt, and 100-ml samples from seawater. Samples were preserved in a 0.5% Lugol solution (based on iodine and glutaraldehyde) and stored at 4°C for analysis in the home laboratory. Cell counts were performed with an inverted microscope (Leica Leitz DM IL), using 125x–500x magnification, after sedimentation in a cuvette according to Utermohl (1958). Cell volume was converted to carbon after Menden-Deuer and Lessard (2000) and slightly modified by Olenina et al. (2006). No correction was made for potential cell shrinkage due to sample fixation. The following carbon-to-volume relationships were used:

$$\text{Carbon mass } \left(\text{pg C cell}^{-1}\right)$$
$$= 0.288 * \text{cell volume}^{0.811} \text{for diatoms;}$$
$$\text{Carbon mass } \left(\text{pg C cell}^{-1}\right)$$
$$= 0.216 * \text{cell volume}^{0.939} \text{for flagellates; and}$$
$$\text{Carbon mass } \left(\text{pg C cell}^{-1}\right)$$
$$= 0.76 * \text{cell volume}^{0.819} \text{for dinoflagellates.}$$

2.4. Statistical analyses
The significance of seasonal trends in photophysiological and biogeochemical parameters were tested by ANOVA using single factor analyses (**Table 2**). A Spearman correlation test was applied to distinguish significant correlations between the bottom-ice parameters. Differences in pigment ratios and production rates were tested with an unpaired t-test.

3. Results
3.1. Environmental conditions
Ice formation in Hangar Cove was variable over the 4-year study period. In 2013, ice formation started in July, with the first ice core taken in August (**Table 1**). The ice pack disappeared again in September due to strong winds. In 2014, ice build-up only started in the middle of winter due to unsettled weather conditions and strong winds in July. The first core was taken on August 17 (**Table 1**). No full record is available for 2015 due to personnel constraints.

Table 2. Total sea-ice column inventory of chlorophyll a (Chl a) and bottom-ice (5 cm) values for selected pigments, photophysiological and biochemical parameters[a] in Ryder Bay, averaged by month (standard deviation, n value) for samplings between 2013 and 2016. DOI: https://doi.org/10.1525/elementa.2021.00029.t2

Month sampled	Chl a (mg m^{-2})	Chl a (μg L^{-1})	Fuco (μg L^{-1})	Hexa (μg L^{-1})	Allo (μg L^{-1})	dt+dd/ Chl a	POC (mg L^{-1})	POC/Chl a (g/g)	Fv/Fm	α (e$^-$ quanta^{-1})	PO$_4$ (μM)	NO$_2$ (μM)	NO$_3$ (μM)	SiO$_3$ (μM)	DIC (μmol kg^{-1})
April	0.24	1.85	0.72	0.05	0.23	0.01	3.66	1976	0.36	0.16	0.77	0.06	6.66	24.07	n.d.
May	0.82	4.79	2.13	0.09	0.28	0.02	3.00	627	0.53	0.22	0.27	0.04	5.67	20.50	n.d.
June	1.97	2.22	0.65	0.00	0.08	0.00	2.83	1276	0.50	0.22	0.29	0.13	9.02	n.d.	n.d.
July	0.18 (0.20, 3)	1.05 (0.87, 4)	0.25 (0.48, 4)	0.00 (0.00, 4)	0.09 (0.04, 4)	0.01 (0.02, 4)	1.79 (1.26, 3)	1261 (357, 3)	0.56	0.24	0.12 (0.07, 2)	0.07 (0.02, 2)	8.57 (0.73, 2)	18.20 (5.68, 2)	829
August	0.24 (0.19, 3)	1.73 (2.54, 8)	0.20 (0.26, 8)	0.07 (0.13, 8)	0.35 (0.61, 8)	0.02 (0.03, 8)	1.02 (0.74, 2)	1537 (287, 3)	0.40 (0.17, 5)	0.15 (0.16, 5)	0.25 (0.21, 4)	0.07 (0.01, 4)	7.26 (0.45, 4)	18.05 (5.36, 4)	464
September	1.97 (1.70, 6)	9.36 (22.51, 9)	3.61 (8.84, 9)	0.05 (0.10, 9)	1.33 (3.26, 9)	0.02 (0.02, 9)	1.52 (0.45, 3)	2348 (1263, 3)	0.22 (0.07, 10)	0.10 (0.08, 5)	0.44 (0.22, 6)	0.10 (0.04, 6)	6.76 (1.30, 6)	19.15 (5.21, 6)	480
October	4.99 (2.00, 5)	19.71 (27, 7)	10.03 (12.62, 7)	0.11 (0.16, 7)	2.07 (5.22, 7)	0.03 (0.01, 7)	4.12 (1.72, 2)	202 (230, 2)	0.29 (0.06, 8)	0.10 (0.05, 6)	0.36 (0.35, 5)	0.08 (0.04, 5)	5.15 (1.63, 5)	12.30 (4.11, 5)	438
November	6.37 (2.00, 7)	53.59 (34.93, 9)	31.55 (22.78, 9)	0.08 (0.11, 9)	0.23 (0.20, 9)	0.06 (0.04, 9)	4.44 (2.62, 5)	70 (40, 5)	0.34 (0.01, 11)	0.12 (0.07, 11)	0.30 (0.35, 8)	0.05 (0.06, 9)	4.59 (3.53, 9)	7.35 (2.12, 9)	327 (39, 3)
December	22.55 (23.66, 6)	290.6 (286.8, 6)	176.3 (174.6, 6)	0.55 (0.70, 6)	0.10 (0.10, 6)	0.14 (0.09, 6)	10.49	10	0.41 (0.01 8)	0.11 (0.05, 8)	0.17 (0.32, 6)	0.03 (0.04, 6)	2.91 (4.19, 6)	7.95 (2.58, 6)	158 (40, 5)
ANOVA[b]	<0.01	<0.05	<0.1	<0.001	<0.001	<0.001	<0.001	<0.001	<0.001	<0.001	<0.001	<0.001	<0.001	<0.05	<0.001
Years[c]	2013–2016	2013–2016	2013–2016	2013–2016	2013–2016	2013–2016	2016	2016	2013–2014, 2016	2013–2014, 2016	2014, 2016	2014, 2016	2014, 2016	2014, 2016	2014, 2015

[a] Fucoxanthin (Fuco), 19'hexanoyloxyfucoxanthin (Hexa), alloxanthin (Allo), diato- plus diadinoxanthin (dt+dd), particulate organic carbon (POC), maximum quantum yield of photosynthesis (Fv/Fm), light affinity (α, electrons quanta^{-1}), and dissolved inorganic carbon (DIC).

[b] Significance of differences between months.

[c] For sampling schedule, see Table S1.
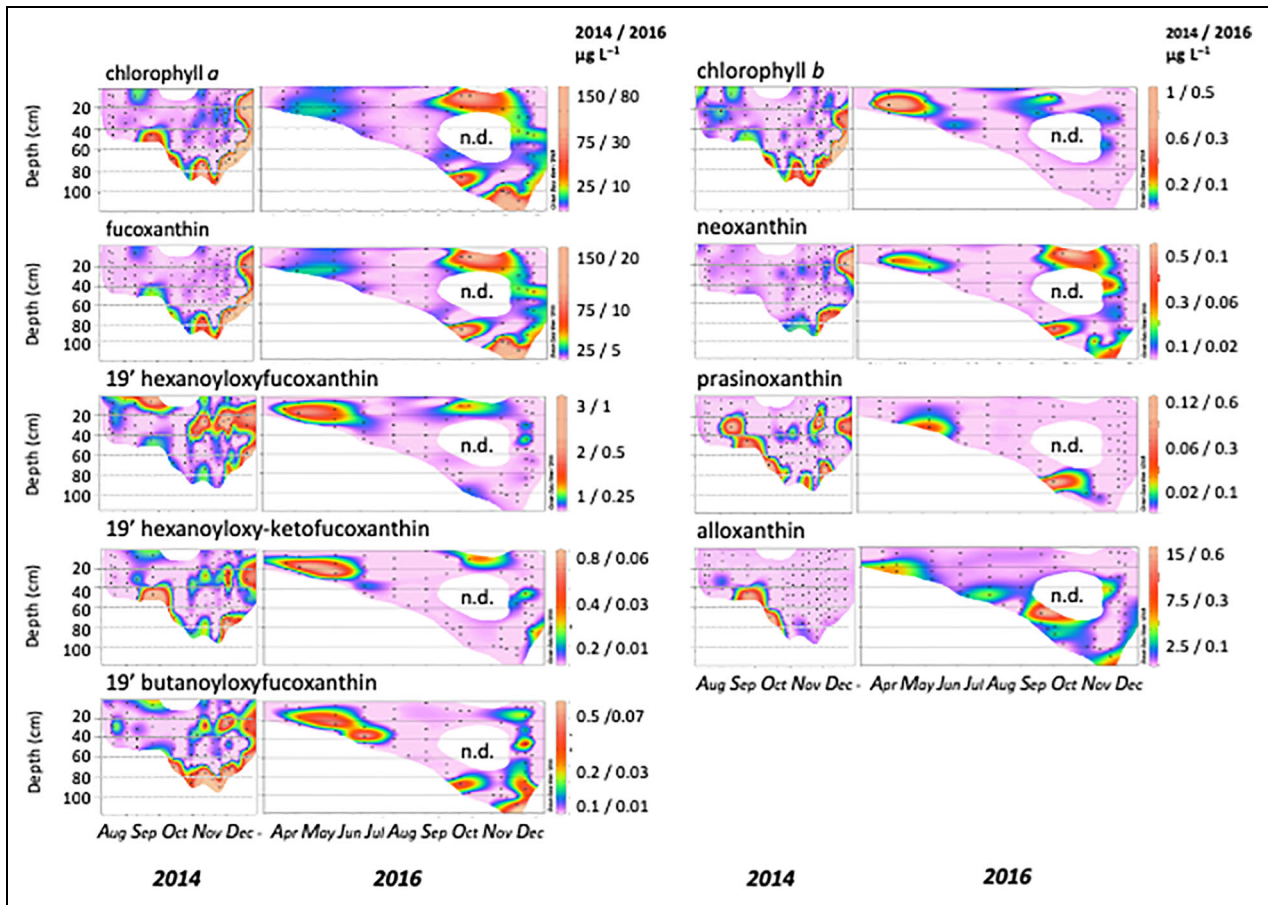
Figure 2. Time series of algal pigments (µg L⁻¹) in sea ice of Hangar Cove. In 2014, ice formation did not start until August, whereas ice formation had already started in April in 2016. Melting events in October–November resulted in slush layers near the surface that could not be sampled accurately. In 2014, the plot for alloxanthin is skewed by high bottom values in October. In 2016, not all interior layers were sampled for pigment analyses (n.d.). DOI: https://doi.org/10.1525/elementa.2021.00029.f2

The most extended time series was sampled in 2016, when the first ice core was taken on April 22 and the last on December 19. Ice thickness gradually increased over winter and spring. At the end of November 2016, the ice reached a maximum depth of 110 cm, after which ice melt commenced (see **Figure 2** and Table S1 for the development of ice thickness). In 2014 and 2016, melt events were recorded in October–November which were followed by refreezing. Snow cover thickness was between 5 and 10 cm, with brief episodes of more than 20 cm (Table S1).

3.2. Algal species succession
3.2.1. In ice
In 2014 and 2016, microalgae were observed in the bottom layers throughout the whole ice period (**Table 2**, **Figure 2**). Bulk-ice concentrations were lowest in autumn and winter with a minimum of 0.2 mg chl a m⁻² in July. Chl a increased rapidly from September onwards, especially in the bottom-ice layers. In December 2014, very high biomass was recorded in bottom sections with maximum concentrations of more than 700 µg Chl a L⁻¹. In 2016, sampling was terminated in early December due to deteriorating ice conditions, when Chl a amounted to 42 µg Chl a L⁻¹.

Algal pigment fingerprints revealed distinct patterns of seasonality in the sympagic communities (**Figure 2**, **Table 2**). In the early stages of ice formation (August 2014 and April–May 2016), elevated signals of 19'hexanoyloxyfucoxanthin (Hexa), 19'hexanoyloxy-ketofucoxanthin (Keto), 19'butanoyloxyfucoxanthin (Buta), chlorophyll b (Chl b), alloxanthin (Allo) and fucoxanthin (Fuco) indicated that a mixture of algal species was incorporated in the sea ice (**Figure 2**). From September onwards, algal biomass increased in the bottom-ice sections. These communities again consisted of a mixture of species, as indicated by the variety of pigments, but the high concentrations of Fuco, presented as multi-year average values, showed that diatoms were most dominant (**Figure 2**; multi-year averages in **Table 2**). In 2014, a melt event in October, followed by refreezing, resulted in an intrusion layer that was colonized by flagellate species marked by Hexa, Chl b, neoxanthin (Neo) and prasinoxanthin (Prasino) (**Figure 2**). This layer stayed visible until the end of the ice season. Flooding events in September–October 2016 were marked by high concentrations of Fuco, Hexa and Neo. The large biomass increases in the bottom-ice layers, recorded from November onwards, were again dominated by diatoms, marked by Fuco.

Microscopic analyses aligned with the pigment patterns described and provided further details on the seasonal succession of microalgae in bottom sea ice in 2014. Major patterns were discerned when all counts were taken to determine group-specific dynamics (**Figures 3** and **4**). In winter and early spring, the bottom communities consisted of a mixture of algal groups. At the end of spring, the bottom of the sea ice was colonized by typical ice algal species such as *Amphiprora kufferathii, Berkeleya* sp. and *Pleurosigma* sp. (**Figure 3**). Various *Nitzschia* species were also present. These diatoms made up most of the total carbon pool. Flagellate species like *Pyramimonas* spp. (prasinophyte) and cryptophytes were also abundant but contributed less to the carbon pool. In December, the warming ice was invaded by various algal species (**Figure 4**). This invasion resulted in mixed algal communities, including centric diatoms and various flagellates, like *Phaeocystis antarctica* (**Figures 3** and **4**). In 2014, additional samples showed the presence of *P. antarctica* also in surface and interstitial layers (Table S2).

The algal community composition in sea ice of Ryder Bay was quite variable (**Figure 5**). Similar to the bottom-ice layer in Hangar Cove (**Figure 4**), the community consisted of mixed algal groups. High concentrations of Fuco, Hexa and Allo indicated the presence of diatoms, flagellates and cryptophytes, respectively (**Figure 5a**). Microscopic observations further showed that pennate diatom, cryptophytes and prymnesiophytes were most dominant (**Figure 5b**). Unlike the sea ice in Hangar Cove, centric diatoms were absent in the bottom layers of the ice in Ryder Bay. Station C was most outstanding, with a strong domination by cryptophytes observed in the bottom-ice community.

3.2.2. Under-ice and pelagic communities
The algal species composition in seawater differed from the species composition in sea ice. Seawater sampled at the Rothera Time Series station showed that during the initial stages of ice melt in November–December 2014 and 2016, the average ($\pm$ standard deviation) Hexa/Fuco ratio was 0.49 ($\pm$ 0.31) (Table S3). This average was significantly higher (p < 0.0001, t-test) than the average ratio of 0.07 ($\pm$ 0.06) that coincided with increasing algal biomass in late December.

Microscopic observations showed a shift in algal communities after the onset of ice melt. In November and December 2014, the under-ice and seawater communities were dominated by flagellate species like the haptophytes *Phaeocystis antarctica* and *Chrysochromulina* sp., and unidentified cryptophyte species (**Figure 3**). These flagellate species dominated not only in cell numbers, but also in carbon contribution. None of the typical sympagic pennate diatoms like *Amphiprora* and *Berkeleya* thrived in the pelagic environment, contributing little to the organic carbon pool (**Figure 3**). The pelagic bloom in December 2013–January 2014 consisted of the centric diatom *Chaetoceros* spp. Observations in 2016 confirmed these general patterns (Table S4): under-ice communities were dominated by small pennates and flagellates, and the seawater

was dominated by cryptophytes, where typical sympagic species like *Amphiprora* were absent.

3.3. Biogeochemistry and photophysiology
A full record of POC in bottom-ice samples from 2016 showed a minimum from July to August, followed by a gradual increase towards December (**Table 2**). The ratio of POC/Chl a was high in winter and gradually declined in spring, to a minimum of 10 in December 2016. In 2014, POC samples were taken in December only. These data provided a clear picture of the increase in δ^{13}C-POC over the course of the month (**Figure 6**). This increase related significantly to the increases in Chl a and POC (p < 0.05, t-test). In early December, surface values for δ^{13}C-POC were close to −20‰ and increased to −10‰. The δ^{13}C-POC in the bottom layer increased to nearly zero (**Figure 6**).

Gross production rates, as obtained from ^{13}C-incorporation experiments, varied between communities (**Table 3**). In 2014, ice-associated communities were size-fractionated, which resulted in a smaller fraction that mainly consisted of small species of *Navicula, Nitzschia, Fragillariopsis, Phaeocystis, Chrysochromulina* and unknown flagellates, and a larger fraction that mainly consisted of *Berkeleya adeliensis*. The average P^C_{max} for the smaller cell fraction was 0.018 (h^{-1}), which was significantly higher (p < 0.05, t-test) than the P^C_{max} of 0.014 (h^{-1}) recorded for larger cells. In 2016, the average P^C_{max} for communities attached to the bottom ice measured 0.011 (h^{-1}) (**Table 3**). Bottom-ice values for carbon and Chl a were used to calculate the photosynthetic capacity (P_{max}), attaining production rates of 2.52 and 5.87 mg C mg^{-1} Chl a h^{-1} in 2014 and 2016, respectively. Net community growth rates calculated based on the increase in Chl a in bottom ice ($\mu^{Chl\ a}$) were 0.092 d^{-1} ($r^2 = 0.82$) and 0.067 d^{-1} ($r^2 = 0.92$) in 2014 and 2016, respectively. In both 2014 and 2016, E_k was around 25 μmol photons m^{-2} s^{-1}.
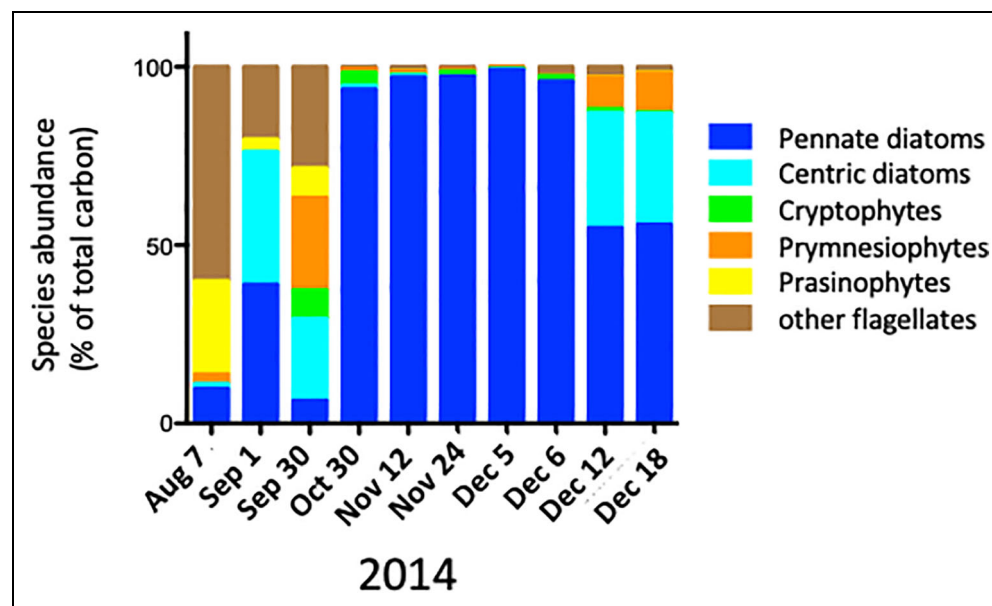
Concentrations of the macronutrients PO_4, NO_3 and silicic acid were high during ice formation in autumn (**Table 2**). Silicic acid in bottom-ice layers declined over time, whereas PO_4 and NO_3 were more variable, with apparent replenishment from underlying seawater in mid-winter. NO_2 concentrations were highest in mid-winter. Concentrations of NO_3, PO_4 and silicic acid declined again from September onwards. The DIC signal correlated significantly with the concentrations in NO_3 and PO_4 (**Table 4**), and declined from August onwards to less than 100 μmol kg^{-1} (**Table 2**) as described in more detail by Jones et al. (2022).

High values for Fv/Fm > 0.6 were measured in winter and early spring 2014 (**Figure 7a**, **Table 2**). Towards summer, Fv/Fm declined in interior and bottom communities, and simultaneously the pool of xanthophyll pigments, diatoxanthin (dt) plus diadinoxanthin (dd), increased (**Figure 7b**). By the end of November, dt+dd/Chl a was > 0.4 in the upper interior ice. Light affinity α was highest end of winter and early spring (**Figure 7c**), and positively correlated with NO_3 concentration (**Table 4**). The light affinity decreased over the season, except for high values at the

		In Ice										Under Ice		Seawater - 5 m						References - Sea ice	
Class	Species	April	May	Sept		Oct		Nov		Dec		Dec		Nov		Dec		Jan			
				cells	carbon	cells	carbon	cells	carbon	cells	carbon	cells	carbon	cells	carbon	cells	carbon	cells	carbon	Antarctic	Arctic
Dinophyceae	*Amphidinium crassum*		+	<1	1															2, 3	4
	Amphidinium sphenoides					<1	<1					<1	<1			<1	<1	<1	<1		
	Gymnodinium cf. ostenfeldii															1	5			8	4
	Gymnodinium/Gyrodinium sp.					<1	<1					<1	<1	2	7	<1	1	1	2	2, 3	6, 7, 11
	Gymnodinium/Karenia sp.		+					<1	1			<1	4			<1	1				
	Gyrodinium cf. lachryma/spirale											<1	9			<1	<1	1	1	2	
	Heterocapsa sp.							<1	1							1	3				7, 9, 11
	Karenia sp.															1	5	1	1		9
	Katodinium glaucum					<1	<1	<1	<1			<1	1			<1	<1	<1	<1		9
	Peridinilales	+														<1	<1				9
	Polarella glacialis													<1	5						7
	Prorocentrum							<1	<1											2, 3	9
	Protoperidinium											<1	1			<1	<1	<1	1	2, 3	6, 7, 9, 11
	Scripsiella/Peridiniella sp.					<1	<1	<1	1			<1	<1			<1	1	<1	1		6, 9
Bacillariophyceae	*Amphiprora kufferathii (p)*			<1	22	4	45	1	19	<1	5	3	40			<1	<1	<1	<1	1, 2, 8, 10, 12	4
	Berkeleya adeliensis (p)					9	14	14	40	46	86	1	3							2, 10, 12	
	Biddulphia aurita v. obtusa (c)							<1	<1			<1	<1							2	
	Chaetoceros sp. (c)	+										1	1	1	3	50	57	38	65	1 - 3	4, 6, 7, 9, 11
	Corethron sp. (c)											<1	1	7	27	<1	11	<1	2	1 - 3, 8, 10	
	Cylindrotheca closterium (p)			<1	1	<1	<1	<1	<1			<1	<1			<1	<1	<1	<1	10	4 - 7, 9, 11
	Eucampia antarctica (c)					<1	<1					<1	8			<1	<1	<1	<1	1 - 3	6, 9
	Fragillariopsis cylindrus/curta (p)			<1	<1	2	1	<1	<1			<1	<1	<1	<1			<1	<1	2, 3, 10	5 - 7, 9, 11
	Fragillariopsis kerguelensis (p)			<1	1	8	5					<1	<1					<1	<1		
	Fragillariopsis sp. (p)		+	<1	<1	5	1	<1	<1	<1	<1	<1	<1	<1	<1	<1	<1	<1	<1	3	7
	Navicula sp. (p)			<1	<1	4	2	2	2	1	<1	<1	<1			<1	<1	<1	<1	2, 8, 10, 12	4 -7, 9, 11
	Nitzschia spp. (p)			11	6	15	20	7	25	29	7	4	4	2	2	5	2	16	6	1 - 3, 8, 10	4 -7, 9, 11
	Plagiotropus gaussii (p)			<1	12	<1	<1					<1	<1	<1	4	1	1	<1	1	3, 10	9, 11
	Pleurosigma sp. (p)			<1	8	1	2	<1	3	<1	<1	<1	<1							2, 3, 8	5, 6, 9, 11
	Proboscia alata (p)							<1	<1			<1	2			<1	<1	<1	2	3	6
	Pseudo_nitzschia (p)		+															<1		3, 10, 12	4, 6, 7, 9, 11
	Thalassiosira sp. (c)							<1				<1	<1			<1	<1	<1	<1	1 - 3	5 -7, 9, 11
	Trichotoxon reinboldii (p)			<1	<1																
Cryptophyceae	*Cryptophytes*		+			4	3	1	1	<1	<1	5	4	2	2	6	4	1	1	2, 10	4, 7, 9, 11
Prymnesiophyceae	*Phaeocystis antarctica*					7	1	2	<1	<1	<1	5	2	15	9	6	1	5	1	1 - 3, 8	9
	Chrysochromulina sp.					1	<1	<1	<1			6	6	19	17	10	5	2	1	2	7
Prasinophyceae	*Pyramimonas sp.*		+	4	3	<1	<1	<1	<1			1	1	3	6	<1	<1	1	<1	2, 3, 8	7, 9, 11
	Micromonas sp.													7	1						9
Raphidophyceae	*Raphidophyte*			8	15	<1	<1	<1	2	<1	<1	<1	<1								7, 9

Figure 3. Species composition in bottom sea ice (5 cm), under ice and seawater in 2014. The abundance of algal species is presented as percentage of total cell numbers and organic carbon. In ice in April and May, only qualitative scores, presented as positive observations (+), were available. Only species that occur in 3 or more ice cores are presented, which together include 50–70% of total carbon and cells numbers. Unidentified flagellates and pennate diatoms account for the remaining part. References refer to publications that mention the same sympagic species. Green shading indicates 2–10% of total contribution; red, > 10% of total contribution. Species were determined in Ryder Bay. Many Arctic observations refer to Arctic subspecies. The Bacillariophyceae included pennate (p) and centric (c) diatoms. References: (1) Garrison et al. (1987); (2) Garrison (1991); (3) Garrison et al. (2005); (4) Horner and Schrader (1982); (5) Kudryavtseva et al. (2017); (6) Melnikov et al. (2002); (7) Mundy et al. (2011); (8) Perrin et al. (1987); (9) Ratkova and Wassmann (2005); (10) Riaux-Gobin et al. (2013); (11) Rozanska et al. (2009); (12) Saggiomo et al. (2017). DOI: https://doi.org/10.1525/elementa.2021.00029.f3

Downloaded from http://online.ucpress.edu/elementa/article-pdf/10/1/00029/497095/elementa.2021.00029.pdf by guest on 17 June 2022

Figure 4. Seasonal development of sea-ice algal classes derived from microscopic analyses in 2014. Samples were taken from bottom sections (5 cm) of ice cores in Hangar Cove. Data are based on the detailed **Figure 3**, presented as a percentage of total carbon (n = 1 per sampling date). DOI: https://doi.org/10.1525/elementa.2021.00029.f4

very surface. Lowest values were recorded in bottom communities, in November and December (**Figure 7c**).

4. Discussion

Sea ice during springtime can be extremely rich in algal biomass and biodiversity. The highest diversity has been recorded for diatoms, with more than 500 taxa described (Arrigo, 2014; Van Leeuwe et al., 2018). Despite numerous studies on sea-ice algal communities, insight into the details of the community structure at the species level remains limited, and a precise description of the succession of sympagic species during the process of ice melt is not available. The microscopic data from 2014 and 2016 revealed how the link between the sea-ice and pelagic systems depends strongly on the species composition of the sympagic community. A clear picture emerges for Antarctic sea ice, showing that after ice melt two separate episodes can be discerned that define the link between the sea ice and seawater, with a major role for chrysophytes, cryptophytes and haptophytes. The new data presented here are interpreted in the context of previous studies, which show that the patterns observed in Ryder Bay were characteristic over the wider sea-ice domain.

4.1. In-ice dynamics

Ice formation in Ryder Bay is linked to the freezing of wider Marguerite Bay, the onset of which varies from April to June (Fritsen et al., 2008). Over the period of 2013–2017, the average Chl a inventory ranged between 0.18 and 22.55 mg m^{-2}, and bottom sea-ice concentration varied between 0.02 µg in winter (July 2015) and 745 µg Chl a L^{-1} in summer (December 2014). These ranges are typical for Antarctic landfast ice (Meiners et al., 2018). The dynamics in biomass were linked to changes in algal

species composition. This phenology can be explained by differences in photophysiological characteristics, as well as by distinctive metabolic strategies.

4.1.1. Species succession

During ice formation in 2014, a mixture of algal species present in the seawater was incorporated in sea ice, including dinoflagellates, diatoms and various autotrophic flagellates (**Figure 3**). In winter, low light conditions select for specific groups like cryptophytes, which are most likely supported by a heterotrophic or mixotrophic lifestyle (van Leeuwe et al., 2018). Increased heterotrophic activity was shown by elevated NO$_2$ concentrations that are indicative of remineralization processes. Dinoflagellates and chrysophytes can survive the winter by cyst formation (Stoecker et al., 1998). In contrast, the centric diatoms that were incorporated during ice formation did not sustain over winter (**Figure 4**). Pennate diatoms seem more flexible and endure the more extreme conditions in winter by varying strategies of energy storage and cyst formation (Garrison et al., 2005; Leu et al., 2015; Van Leeuwe et al., 2018). Indeed, of the mixed algal autumn community in Ryder Bay sea ice, mostly the smaller opportunistic species like *Fragillariopsis* spp. and *Pyramimonas* spp. survived over winter.

In spring 2014 and 2016, *Pyramimonas* spp., raphidophytes and pennate diatoms like *Nitzschia* spp. were the first to profit from increasing irradiance and rapidly increased in biomass. Their early increase in abundance may be explained by a high affinity for light (Cota and Sullivan, 1990; Rozanska et al., 2009). In November, the reappearance of the centric diatom *Proboscia alata* (**Figure 3**) was most likely associated with the infiltration of seawater, facilitated by the relatively warm and porous
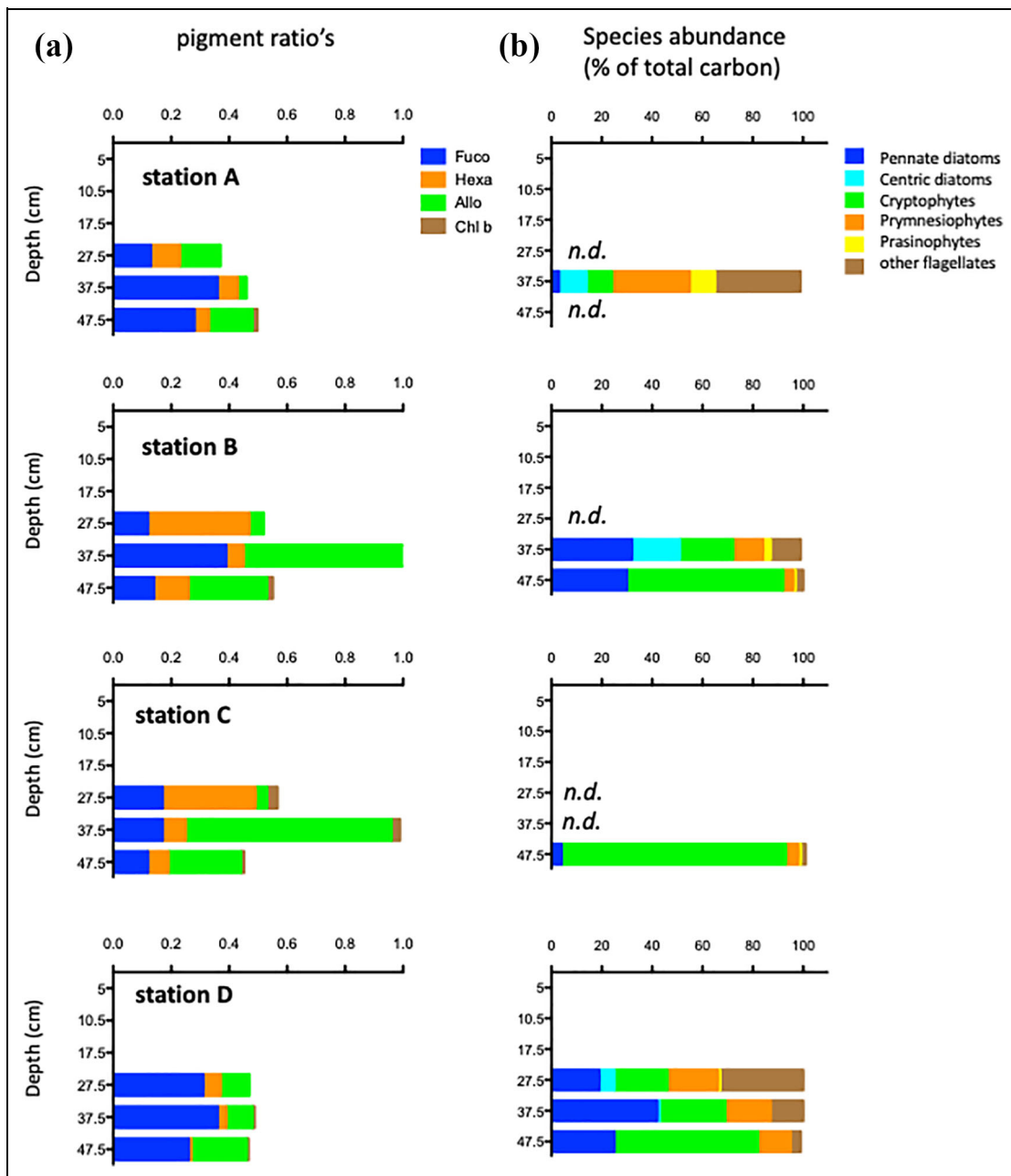
Figure 5. Distribution of algal classes in bottom sea ice along a transect in Ryder Bay. On September 30, 2014, 4 stations were sampled. Bottom sections (5 cm) were analyzed, showing (a) algal pigment ratios to Chl *a* and (b) community composition based on microscopic analyses, presented as a percentage of total carbon; n.d. indicates no data. DOI: https://doi.org/10.1525/elementa.2021.00029.f5

structure of sea ice in Ryder Bay (Fritsen et al., 2008). The spring phenology in Ryder Bay was very similar to findings in East Antarctica (Riaux-Gobin et al., 2013), with *Amphiprora kufferathii* thriving early in the season and *Nitzschia* spp. and *Fragillariopsis* appearing later. The succession was completed by the strand-forming pennate diatom *Berkeleya adeliensis,* which is apparently the best at maintaining itself in the changing structure of the melting sea ice.

4.1.2. Photophysiology and biogeochemistry
The build-up of algal biomass in spring was controlled by light and nutrient conditions (see **Table 4** for correlations). The high ratio of dt+dd/Chl *a,* with values > 0.4

in interior ice at the end of November and early December, was associated with a decline in light affinity α. These characteristics are typical for communities adapted to high light (Alou-Font et al., 2013). In contrast, bottom communities were likely controlled by a combination of light and nutrient limitation. In winter 2016, extremely high POC/Chl *a* ratios were recorded (**Table 2**), whereby part of the carbon most likely consisted of organic material not associated with healthy microalgae, such as detritus, bacterial communities and extracellular polymeric substances (Riedel et al., 2008). Algal growth was initiated in October and November, with gross production rates (P_{max}) between 2.52 and 5.87 mg C mg^{-1} Chl *a* h^{-1} that
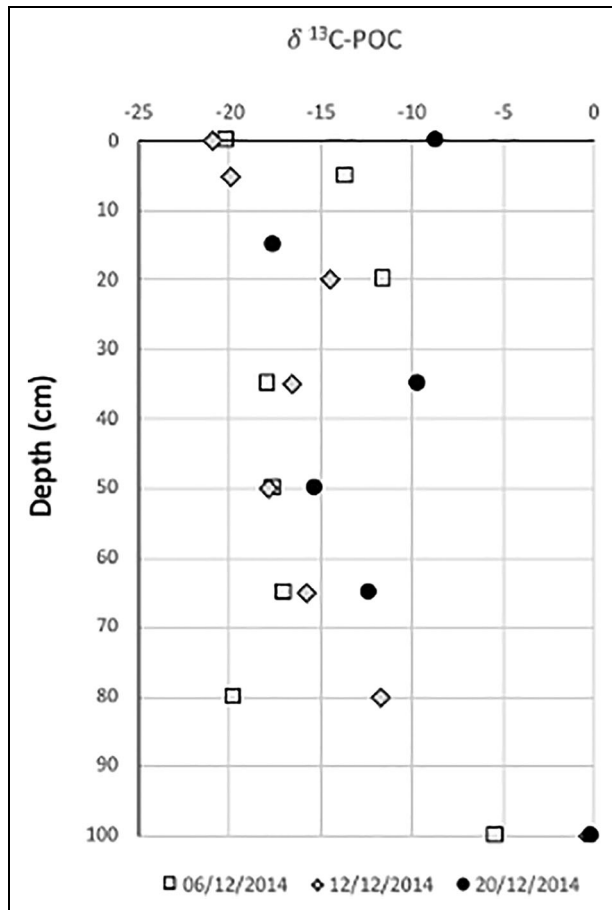
Figure 6. Development of δ^{13}C-POC in sea ice over the course of December 2014. All ice cores were taken at one location in Hangar Cove (n = 1 per sampling date). DOI: https://doi.org/10.1525/elementa.2021.00029.f6

agreed well with other findings for Antarctic sympagic bottom communities (McMinn et al., 2010; Arrigo et al., 2014; Van Leeuwe et al., 2018). The growth of bottom-ice algal communities resulted in rapid chlorophyll synthesis relative to the more stagnant carbon pool, with an ensuing decrease in POC/Chl a. The continuing decline of the ratio over summer indicated increased Chl a, which was considered due to photoacclimation towards lower light intensities, most likely as a result of self-shading within the dense biolayers (Lizotte and Sullivan, 1992; Arrigo et al., 2014). The depletion of inorganic macronutrients may further explain the seasonal decline in photosynthetic activity (Selz et al., 2018a). Across a number of studies, the photoadaptive status of bottom communities appears remarkably consistent, with E_k, averaging about 25 µmol photons m^{-2} s^{-1}, indicating light adaptation to intermediate light levels (Palmisano et al., 1987; Michel et al., 1988; Mangoni et al., 2009; Arrigo et al., 2014). The high values for Fv/Fm and α in November and December 2014, observed at the very surface layer (**Figure 7**), might be explained by refreshening of the algal communities by seawater flooding, but, unfortunately, no observations are available to support this possibility.

The rapid increase in biomass in late spring–early summer was reflected in marked decreases in total dissolved inorganic carbon (for detailed discussion, see Jones et al., 2022). The enrichment of ^{13}C-POC in sea ice coincided with CO_2 depletion in the semi-closed sea-ice matrix, where CO2 exchange is limited and biological drawdown intense. The enrichment was most pronounced in the bottom-ice layers, where it links to the high build-up of algal biomass. A similar link between POC depletion and ^{13}C-POC was observed in surface-ice communities in the Amundsen Sea (Arrigo et al., 2014). Subsequent enrichment of δ^{13}C-POC in seawater may be considered an indication of sea-ice melt, as previously shown in Ryder Bay (Henley et al., 2012), wider Marguerite Bay (Stefels et al., 2018) and Prydz Bay (Zhang et al., 2014).

4.2. Seeding link between sea ice and seawater
The seeding potential of sea ice appeared to be species-specific. A detailed examination of the data showed that two separate phases may be distinguished in the pelagic environment: an initial increase in ice-associated algae that were dominated by flagellates, followed later by an increase in diatoms. This study revealed that only the first biomass increase was linked to the release of sympagic algae seeding the water column (**Figure 3**), whereas summer pelagic algal blooms appear to be controlled by hydrographic conditions.

The genuine seeding event that was associated with sea-ice melt originated in the release of flagellates like cryptophytes and prymnesiophytes, which inhabited the sea ice and also thrived under the ice. These findings confirm previous observations in the coastal zone within and outside Ryder Bay, where flagellates were the first to profit from the improved conditions in spring (Stefels et al., 2018; van Leeuwe et al., 2020). Of the mixed algal communities that inhabit the bottom-ice layers, many species do not survive the transition to open seawater. The species that remain vital after release from the ice will have the highest photoflexibility and be capable of dealing with the likely abrupt change in light conditions. Especially shade-adapted pennate diatoms that often dominate the bottom-ice communities respond poorly to exposure to the generally higher light conditions in open seawater, whereas flagellate species apparently adapt very well to changing light conditions (McMinn, 1996; Kropuensky et al., 2010; Van Leeuwe et al., 2020). In line with these observations, highest growth rates were recorded for the smallest algal fraction (**Table 3**), which included many flagellate species. The importance of photoflexibility, and the associated light history of sympagic communities, is furthermore reflected in an earlier study on photophysiology and carbon metabolism of sea-ice algae in pack ice of the Weddell Sea. This study showed that species from bottom communities disappeared upon ice melt, whereas communities from interior layers that were adapted to intermediate light intensities were more successful in the water column (Gleitz and Kirst, 1991).

In 2014 in Ryder Bay, the pelagic biomass peak consisted of cells of *Chaetoceros* sp. This species did not inhabit the sea ice. In Antarctic coastal waters, important pelagic blooms are often formed by centric diatoms like

Table 3. Photosynthetic parameters[a] for algal communities associated with bottom sea ice. DOI: https://doi.org/10.1525/elementa.2021.00029.t3

Sample Year, Type	P^C_{max} [b] (h^{-1})	E_k (μmol photons $m^{-2} s^{-1}$)	POC[c] $(mg L^{-1})$	Chl a[c] $(\mu g L^{-1})$	P_{max}[d] $(mg C mg^{-1}$ Chl $a^{-1} h^{-1})$	$\mu^{Chl\ a}$ (d^{-1})
2014, < 300 μm	0.018 (0.001, 6)	26	na[e]	na	na	na
2014, > 300 μm	0.014 (0.001, 6)	23	na	na	na	na
2014, averaged	0.016[f]	na	76	483	2.52	0.092
2016, attached	0.011 (0.002, 4)	22	8	15	5.87	0.067

[a] Maximum growth capacity (P^C_{max}), index for photoadaptation (E_k), maximum photosynthetic capacity (P_{max}), and net community growth rate ($\mu^{Chl\ a}$).

[b] Average value (standard deviation, n value).

[c] Average value for particulate organic carbon (POC) and chlorophyll a (Chl a) in bottom sea ice (5 cm) in November–December (n = 3).

[d] P_{max} was calculated as P^C_{max} * POC/Chl a (single value).

[e] Not available.

[f] Average value of the fractions <300 μm and >300 μm.

Thalassiosira and *Chaetoceros*, which are absent from the foregoing sea-icescape (Garrison et al., 1987; Rozema et al., 2017; Van Leeuwe et al., 2020). Pennate diatoms like *Nitzschia* sp. and *Fragillariopisis* sp. were omnipresent and may inhabit sea ice as well as seawater, but they are not the "seed" that develop into large pelagic blooms. Several studies have indicated that the typical ice-algal species like *Amphiprora kufferathii* and many *Nitzschia* species cannot sustain the sudden change in light conditions (McMinn, 1996; Mangoni et al., 2009; Kvernvik et al., 2020). The sympagic species disappear from the water column and are replaced by other species that profit more from new hydrographic conditions in spring and summer, specifically the stabilization of the water column which provides nutrients and an optimal light climate (Smith and Nelson, 1990; Lancelot et al., 1991; Rozema et al., 2017).

4.3. Broader context

To investigate the extent to which the findings in Ryder Bay have wider relevance across different ice types and geographic regions (see references in **Figure 3**), we have contextualised our results with those from previous studies. Evaluating them in light of the seeding mechanism presented here, we find that previous studies revealed not only many similarities in species composition in the ice, but also that the seeding link between sea ice and seawater as recorded in Ryder Bay has parallels in various other Antarctic regions (Stoecker et al., 1998; Rozanska et al., 2009; Selz et al., 2018a). In all of these studies, the first ice-melt bloom contained a variety of flagellates, including crypto-, chryso-, prymnesio- and prasinophyceae like *Pyramimonas* spp. Most noticeable is the omnipresence of the haptophyte *Phaeocystis antarctica*, which has often been observed underneath sea ice and in open water during early ice melt in East Antarctica and the Weddell Sea (Garrison et al., 1987; Perrin et al., 1987; Scharek et al., 1994; McMinn, 1996; Riaux-Gobin et al., 2013).

Many Arctic studies also closely matched the findings in Antarctica, with a phenology in sympagic algae analogous to the findings in Ryder Bay, and a similar seeding potential for flagellate species (see Van Leeuwe et al., 2018, and refs therein). The results of an extensive study in the Canadian Beaufort Sea on species succession in sea ice corroborates our study; the winter sea ice was dominated by heterotrophic flagellates whereas pennate diatom species with a higher light affinity flourished in spring (Rozanska et al., 2009). Furthermore, centric diatoms like *Thalassiosira* and *Chaetoceros* are mostly ubiquitous in the marine environment, including in the Arctic (Lovejoy et al., 2002; Ratkova and Wassmann, 2005). Some centric species can occur in sea ice, but they arrive later and their appearance seems to be related to intrusion events; they have been considered "allochthonous" to the ice environment (Ratkova and Wassmann, 2005). Similar to the Antarctic, *Nitzschia* spp. are omnipresent in the Arctic (Michel et al., 1993; Melnikov et al., 2002; Ratkova and Wassmann, 2005). Likewise, a dominance of flagellate species, like *Pyramimonas* spp. in the early pelagic blooms, is often observed (Ratkova and Wassmann, 2005; Mundy et al., 2011; Selz et al., 2018a). Algal pelagic blooms that develop later in spring mostly consisted of centric diatom species that clearly flourished better in open water (Horner and Schrader, 1982; Michel et al., 1993; Szymanski and Gradinger, 2016; Selz et al., 2018b). In the Chukchi Sea study by Selz et al. (2018a) not only the composition of the algal community but also biomass was taken into account when evaluating the link between sea ice and seawater: a model was applied that showed that given the limited timespan the increase in centric diatoms that formed the spring pelagic bloom could not have

Table 4. Spearman's rank correlation coefficients and p values for sampled bottom parameters. DOI: https://doi.org/10.1525/elementa.2021.00029.t4

Parameter[a]	Chl a	Fuco	Hexa	Allo	dt+dd/Chl	POC	POC/Chl	Fv/Fm	α	PO$_4$	NO$_2$	NO$_3$	SiO$_3$	DIC
Chl a	–	$p < 0.01$	$p < 0.05$	ns[b]	$p < 0.05$	$p < 0.05$	ns	ns	$p < 0.05$	ns	ns	$p < 0.01$	ns	$p < 0.05$
Fuco	0.97	–	$p < 0.05$	ns	$p < 0.05$	$p < 0.05$	ns	ns	ns	ns	ns	$p < 0.01$	ns	$p < 0.05$
Hexa	0.74	0.71	–	ns	$p < 0.05$	ns	$p < 0.05$	ns	ns	ns	ns	$p < 0.01$	ns	$p < 0.05$
Allo	na[b]	na	na	–	n.s.	ns	ns	$p < 0.05$	$p < 0.05$	ns	ns	ns	ns	ns
dt+dd/Chl	0.82	0.80	0.88	na	–	ns	$p < 0.05$	ns	$p < 0.05$	ns	ns	$p < 0.05$	$p < 0.05$	$p < 0.01$
POC	0.73	0.72	na	na	na	–	$p < 0.05$	ns	ns	ns	ns	ns	ns	ns
POC/Chl	−0.63	−0.63	−0.69	na	−0.69	−0.80	–	ns	ns	ns	ns	ns	ns	ns
Fv/Fm	na	n.a	na	−0.70	na	na	na	–	$p < 0.05$	ns	ns	ns	ns	ns
α	−0.71	−0.66	na	−0.68	−0.70	na	na	0.87	–	ns	ns	$p < 0.05$	ns	ns
PO$_4$	na	na	na	na	na	na	0.60	na	na	–	ns	ns	ns	ns
NO$_2$	n.a	n.a	−0.60	na	na	na	na	na	na	na	–	ns	ns	ns
NO$_3$	−0.93	−0.93	−0.89	na	−0.91	−0.63	0.67	na	0.67	na	na	–	0.67	0.94
SiO$_3$	−0.72	−0.67	na	na	−0.88	na	0.69	na	na	na	na	0.67	–	0.94
DIC	−0.94	−0.83	−0.94	na	−0.99	−0.77	0.83	na	na	na	na	0.94	0.94	–

[a] Chlorophyll a (Chl a), fucoxanthin (Fuco), 19'hexanoyloxyfucoxanthin (Hexa), alloxanthin (Allo), diatoxanthin (dt), diadinoxanthin (dd), particulate organic carbon (POC), maximum quantum yield of photosynthesis (Fv/Fm), light affinity (α, electrons quanta^{-1}), and dissolved inorganic carbon (DIC).

[b] Not significant (ns; defined here as p value > 0.1) or not available (na).
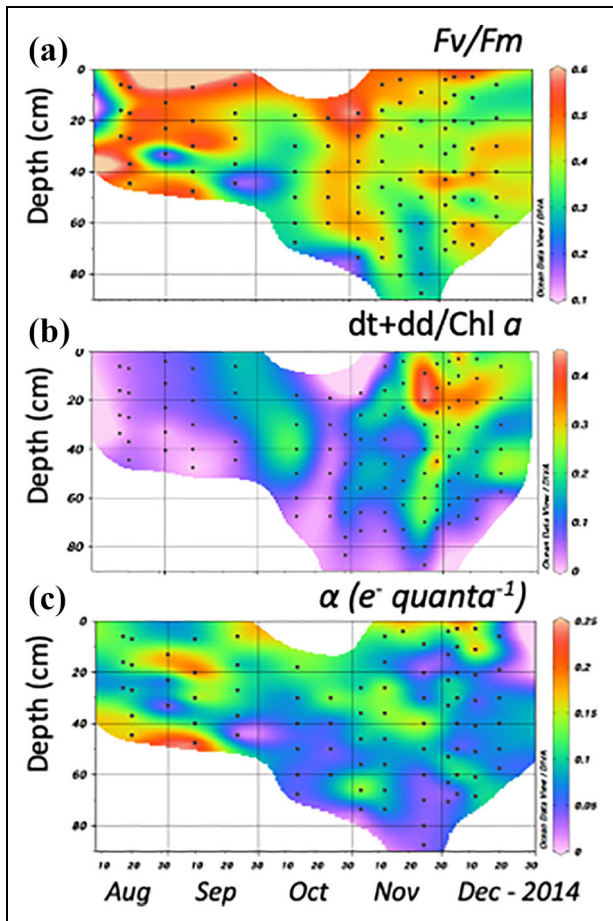
Figure 7. Seasonal patterns in algal photophysiology in sea ice of Hangar Cove in 2014. A time series is shown for (a) maximum quantum yield of photosynthesis, Fv/Fm; (b) ratio of diato- plus diadinoxanthin to chlorophyll a, (dt+dd)/Chl a; and (c) light affinity, α (electrons quanta^{-1}) as derived by fluorescence analysis. DOI: https://doi.org/10.1525/elementa.2021.00029.f7

developed from the small seeding community provided by the sea ice.

Although less frequently observed, literature shows that centric diatoms can form an additional seeding reservoir. They appear relatively late in bottom-ice communities. With increasing light intensities in spring, centric species can become dominant over pennate diatoms (Melnikov et al., 2002; Galindo et al., 2014; Campbell et al., 2018). Unlike pennate diatoms, they appear to grow well under high light conditions (Kvernvik et al., 2020) and thus are more likely to be successful as a seeding community. Centric diatoms like *Porosira pseudodenticulata* also frequently inhabit platelet ice, where they profit from high nutrient concentrations and a more beneficial light climate (Lizotte and Sullivan, 1992; Riaux-Gobin et al., 2013). Platelet ice has an open structure and a stronger connection to ambient seawater compared to columnar ice (Arrigo, 2014), which facilitates exchange of algal communities and hence contributes to the seeding capacity of platelet communities (Saggiomo et al., 2017).

4.4. Ecological implications and future predictions

The seeding potential of sea ice appeared to be restricted to smaller flagellate species (and smaller diatoms) that are more opportunistic than larger diatom species. In spring, the first seeding event is easily overlooked as its contribution may be small in terms of biomass. In Ryder Bay, the calculated average net community growth rates of 0.067 and 0.092 d^{-1} are of similar magnitude as the measured specific production rates of 0.014 and 0.018 h^{-1} (**Table 3**), assuming active production over a period of 8–10 h per day. This similarity indicates that little algal biomass was lost from the bottom sea ice. Yet, the seeding component is still of importance for the biogeochemical cycles of the surrounding seawater. The haptophyte *Phaeocystis antarctica* is amongst the algal species that thrive in the MIZ. It is a prominent producer of DMSP, which is the precursor of the climate-active gas DMS (Stefels et al., 2007; Stefels et al., 2018), which, once emitted into the atmosphere, plays an important role in cloud formation.

Sea ice has been thinning, and the sea-ice season shortening, in the Arctic over many decades, with related predictions for Antarctic sea-ice loss in the near future (Maksym, 2019; Roach et al., 2020). In Antarctica, sea-ice snow cover is forecasted to increase, with negative consequences for bottom-ice communities that are controlled by light availability (Jeffery et al., 2020). In spring, ice dynamics will likely become more dynamic, which will result in more dramatic changes in light conditions. Especially flagellate species can be predicted to benefit from the changing conditions. The build-up of biomass in sea ice will become subject to early disruption, implying that bottom communities of pennate diatoms will be lost from the sea-ice bottom at an early stage, whereas centric diatom communities will have less time to develop. The increasingly early release of bottom communities into the seawater will likely be most beneficial to flagellate species like chrysophytes, cryptophytes and the haptophyte *Phaeocystis antarctica*. With a forecast of increasing biomass in the MIZ, primary production will increase in the near future (Jeffery et al., 2020; Van Leeuwe et al., 2020), as will DMS fluxes into the atmosphere. The consequences for carbon fluxes are harder to predict. Whereas diatoms generally contribute the most to carbon drawdown, the wax and wane of *Phaeocystis* blooms has also been associated with large carbon fluxes into the deep ocean (Arrigo et al., 1999). The overall result of changing sea-ice dynamics on carbon fluxes remains uncertain and warrants investigation.

The impact of climate change for higher trophic levels is also hard to predict. In winter, sea-ice algae are the main food source for larval and juvenile krill (Kohlbach et al., 2017). The feeding reservoir for higher trophic levels will be affected with the potential changes in algal species composition. Moreover, an earlier onset of algal blooms might result in a mismatch between trophic levels, with negative consequences for their reproduction (Soreide et al., 2010). Conversely, the role of grazing in shaping the community structure in spring may be important yet is highly understudied (Scharek et al., 1994). Further investigation of secondary production and trophic interactions

is needed in order to better predict the structure and dynamics of sea-ice associated communities in the near future (Lannuzel et al., 2020).

Data accessibility statement
All pigment and carbon data are stored in the GELifes repository: https://doi.org/10.34894/89N73S.

Supplemental files
The supplemental files for this article can be found as follows:

Table S1. Sampling details of ice cores collected between 2013 and 2016. xlsx

Table S2. Distribution of microalgal species composition, expressed in cells/ml. xlsx

Table S3. Chlorophyll a concentrations (Chl *a*) and the ratio of 19'hexanoyolfucoxanthin (HEXA) to fucoxanthin (FUCO) in surface waters of Ryder, during ice melt in spring 2014. xlsx

Table S4. Species composition in bottom sea ice (5 cm), under ice and in seawater in 2016. xlsx

Competing interests
None of the authors have any conflict of interest.

Author contributions

- Contributed to conception and design: MAvL, JS.
- Contributed to acquisition of data: MAvL, MF, ED, J-MR, EMJ, JS.
- Contributed to analysis and interpretation of data: MAvL, J-MR, JS.
- Drafted and/or revised the article: MAvL, MF, ED, J-MR, EMJ, MPM, JS.
- Approved the submitted version for publication: MAvL, MF, ED, J-MR, EMJ, MPM, JS.

References

Alou-Font, A, Mundy, C-J, Roy, S, Gosselin, M, Agusti, S. 2013. Snow cover affects ice algal pigment composition in the coastal Arctic Ocean during spring. *Marine Ecology Progress Series* **474**: 89–104.

Arrigo, KR. 2014. Sea ice ecosystems. *Annual Reviews in Marine Science* **6**: 439–467.

Arrigo, KR. 2017. Sea ice as a habitat for primary producers, in Thomas, DN ed., *Sea ice*, 3rd ed. Oxford, UK: Wiley-Blackwell: 352–369.

Arrigo, KR, Brown, ZW, Mills, MM. 2014. Sea ice algal biomass and physiology in the Amundsen Sea, Antarctica. *Elementa Science of the Anthropocene* **2**: 000028. DOI: http://dx.doi.org/10.12952/journal.elementa.000028.

Arrigo, KR, Robinson, DH, Worthen, DL, Dunbar, RB, DiTullio, GR, VanWoert, M, Lizotte, MP. 1999. Phytoplankton community structure and the drawdown of nutrients and CO_2 in the Southern Ocean. *Science* **283**: 365–367.

Buesseler, KO, Barber, RT, Dickson, M-L, Hiscock, MR, Moore, JK, Sambrotto, R. 2003. The effect of marginal ice-edge dynamics on production and export in the Southern Ocean along 170°W. *Deep-Sea Research II* **50**: 579–603.

Campbell, K, Mundy, CJ, Belzile, C, Delaforge, A, Rysgaard, S. 2018. Seasonal dynamics of algal and bacterial communities in Arctic sea ice under variable snow cover. *Polar Biology* **41**: 41–58.

Cota, GF, Sullivan, CW. 1990. Photoadaptation, growth and production of bottom ice algae in the Antarctic. *Journal of Phycology* **26**: 399–411.

Fritsen, CH, Memmott, J, Stewart, FJ. 2008. Interannual sea-ice dynamics and micro-algal biomass in winter pack ice of Marguerite Bay, Antarctica. *Deep-Sea Research II* **55**: 2059–2067.

Galindo, V, Levasseur, M, Mundy, CJ, Gosselin, M, Tremblay, J-E, Scarratt, M, Gratton, Y, Papakiriakou, T, Poulin, M, Lizotte, M. 2014. Biological and physical processes influencing sea ice, under-ice algae, and dimethylsulfoniopropionate during spring in the Canadian Arctic Archipelago. *Journal of Geophysical Research: Oceans* **119**. DOI: http://dx.doi.org/10.1002/2013JC009497.

Garrison, DL. 1991. Antarctic sea ice biota. *American Zoologist* **31**: 17–33.

Garrison, DL, Buck, KR, Fryxell, GA. 1987. Algal assemblages in Antarctic pack ice and in ice-edge plankton. *Journal of Phycology* **23**: 564–572.

Garrison, DL, Gibson, A, Coale, SL, Gowing, MM, Okolodkov, YB, Fritsen, CH, Jeffries, MO. 2005. Sea-ice microbial communities in the Ross Sea: Autumn and summer biota. *Marine Ecology Progress Series* **300**: 39–52.

Gleitz, M, Kirst, GO. 1991. Photosynthesis-irradiance relationships and carbon metabolism of different ice algal assemblages collected from Weddell Sea pack ice during austral spring (EPOS 1). *Polar Biology* **11**: 385–392.

Grasshoff, K. 1983. Determination of nutrients, in Grasshoff, K, Ehrhardt, M, Kremling, M eds., *Methods of seawater analysis.* Weinheim, Germany: Verlag Chemie: 143–150.

Henley, SF, Annett, AL, Ganeshram, RS, Carson, DS, Weston, K, Crosta, X, Tait, A, Dougans, J, Fallick, AE, Clarke, A. 2012. Factors influencing the stable carbon isotopic composition of suspended and sinking organic matter in the coastal Antarctic sea ice environment. *Biogeosciences* **9**: 1137–1157.

Henley, SF, Schofield, OM, Hendry, KR, Schloss, IR, Steinberg, DK, Moffat, C, Peck, LS, Costa, DP, Bakker, DCE, Hughes, C, Rozema, PD, Ducklow, HW, Abele, D, Stefels, J, Van Leeuwe, MA, Brussaard, CPD, Buma, AGJ, Kohut, J, Sahade, R, Friedlaender, AS, Stammerjohn, SE, Venables, HJ, Meredith, M. 2019. Variability and change in the west Antarctic Peninsula marine system: Research priorities and opportunities. *Progress in Oceanography* **173**: 208–237.

Horner, R, Schrader, GC. 1982. Relative contribution of ice algae, phytoplankton, and benthic microalgae to primary production in nearshore regions of the Beaufort Sea. *Arctic* **35**: 485–503.

Jeffery, N, Maltrud, ME, Hunke, EC, Wang, S, Wolfe, J, Turner, AK, Burrows, SM, Shi, X, Lipscomb, WH, Maslowski, W, Calvin, KV. 2020. Investigating controls on sea ice algal production using E3SMv1.1-BGC. *Annals of Glaciology* **61**(82): 51–72.

Johnson, KM, Sieburth, JM, Williams, PJL, Brandstrom, L. 1987. Coulometric total carbon dioxide analysis for marine studies—automation and calibration. *Marine Chemistry* **21**: 117–133.

Jones, EM, Henley, SF, Van Leeuwe, MA, Stefels, J, Meredith, M, Fenton, M, Venables, H. 2022. Carbon and nutrient cycling in Antarctic landfast sea ice from winter to summer. *Limnology and Oceanography.*

Kohlbach, D, Lange, B, Schaafsma, F, David, C, Vortkamp, M, Graeve, M, Van Franeker, J, Krumpen, T, Flores, H. 2017. Ice algae-produced carbon is critical for overwintering of Antarctic krill *Euphausia superba. Frontiers in Marine Science* **4**. DOI: http://dx.doi.org/10.3389/fmars.2017.00310.

Kropuenske, LR, Mills, MM, Van Dijken, GL, Alderkamp, AC, Berg, GM, Robinson, DH, Welschmeyer, NA, Arrigo, KR. 2010. Strategies and rates of photoacclimation in two major Southern Ocean phytoplankton taxa: *Phaeocystis antarctica* (haptophyta) and *Fragilariopsis cylindrus* (bacillariophyceae). *Journal of Phycology* **46**: 1138–1151.

Kudryavtseva, VA, Belevich, TA, Zhitina, LS. 2017. Diatoms in the ice of Velikaya Salma Strait, the White Sea, before the spring algal bloom. *Hydrobiology* **72**(2): 52–58.

Kvernvik, AC, Rokitta, SD, Leu, E, Harms, L, Gabrielsen, TM, Rost, B, Hoppe, CJM. 2020. Higher sensitivity towards light stress and ocean acidification in an Arctic sea-ice-associated diatom compared to a pelagic diatom. *New Phytologist* **226**: 1708–1724.

Lancelot, C, Billen, G, Veth, C, Becquevort, S, Mathot, S. 1991. Modelling carbon cycling through phytoplankton and microbes in the Scotia-Weddell Sea area during sea ice retreat. *Marine Chemistry* **35**: 305–324.

Lannuzel, D, Tedesco, L, van Leeuwe, MA, Campbell, K, Flores, H, Delille, B, Miller, L, Stefels, J, Assmy, P, Bowman, J, Brown, K, Castellani, G, Chierici, M, Crabeck, O, Damm, E, Else, B, Fransson, A, Fripiat, F, Geilfus, NX, Jacques, C, Jones, E, Kaartokallio, H, Kotovitch, M, Meiners, K, Moreau, S, Nomura, D, Peeken, I, Rintala, JM, Steiner, N, Tison, JL, Vancoppenolle, M, der Linden, FV, Vichi, M, Wongpan, P. 2020. The future of Arctic sea-ice biogeochemistry and ice-associated ecosystems. *Nature Climate Change* **10**: 983–992. DOI: http://dx.doi.org/10.1038/s41558-020-00940-4.

Legendre, L, Ackley, SF, Dieckmann, GS, Gullicksen, B, Horner, R, Hoshiai, T, Melnikov, IA, Spindler, WSRM, Sullivan, CW. 1992. Ecology of sea ice biota. 2. Global significance. *Polar Biology* **12**: 429–444.

Leu, E, Mundy, C, Assmy, P, Campbell, K, Gabrielsen, T, Gosselin, M, Juul-Pedersen, T, Gradinger, R. 2015. Arctic spring awakening—Steering principles behind the phenology of vernal ice algal blooms. *Progress in Oceanography* **139**: 161–170.

Lizotte, MP. 2001. The contributions of sea ice algae to Antarctic marine primary production. *American Zoologist* **41**: 57–73.

Lizotte, MP, Sullivan, CW. 1992. Biochemical composition and photosynthate distribution in sea ice microalgae of McMurdo Sound, Antarctica: Evidence for nutrient stress during the spring bloom. *Antarctic Science* **4**(1): 23–30.

Lovejoy, C, Legendre, L, Martineau, MJ, Bacle, J, von Quillfeldt, CH. 2002. Distribution of phytoplankton and other protists in the North Water. *Deep Sea Research II* **49**: 5027–5047. DOI: http://dx.doi.org/10.1016/S0967-0645(02)00176-5.

Maksym, T. 2019. Arctic and Antarctic Sea ice change: Contrasts, commonalities, and causes. *Annual Review of Marine Science* **11**: 187–213.

Mangoni, O, Carrada, GC, Modigh, M, Catalano, G, Saggiomo, V. 2009. Photoacclimation in Antarctic bottom ice algae: An experimental approach. *Polar Biology* **32**: 325–335.

McMinn, A. 1996. Preliminary investigation of the contribution of fast-ice algae to the spring phytoplankton bloom in Ellis Fjord, eastern Antarctica. *Polar Biology* **16**: 301–307.

McMinn, A, Pankowskii, A, Ashworth, C, Bhagooli, R, Ralph, P, Ryan, K. 2010. In situ net primary productivity and photosynthesis of Antarctic sea-ice algal, phytoplankton and benthic algal communities. *Marine Biology* **157**: 1345–1356.

Meiners, KM, Vancoppenolle, M, Carnat, G, Castellani, G, Delille, B, Delille, D, Dieckmann, GS, Flores, H, Fripiat, F, Grotti, M, Lange, BA, Lannuzel, D, Martin, A, McMinn, A, Nomura, D, Peeken, I, Rivaro,

P, Ryan, KG, Stefels, J, Swadling, KM, Thomas, DN, Tison, J-L, Van Der Merwe, P, Van Leeuwe, MA, Weldrick, C, Yang, EJ. 2018. Chlorophyll-α in Antarctic landfast sea ice: A first synthesis of historical ice core data. *Journal of Geophysical Research: Oceans* **123**: 8444–8459. DOI: http://dx.doi.org/10.1029/2018JC014245.

Melnikov, IA, Kolosova, EG, Welch, HE, Zhitina, LS. 2002. Sea ice biological communities and nutrients dynamics in the Canada Basin of the Arctic Ocean. *Deep Sea Research I* **49**: 1623–1649. DOI: http://dx.doi.org/10.1016/S0967-0637(02)00042-0.

Menden-Deuer, S, Lessard, EJ. 2000. Carbon to volume relationships for dinoflagellates, diatoms, and other protist plankton. *Limnology and Oceanography* **45**: 569–579.

Meredith, MP, King, C. 2005. Rapid climate change in the ocean west of the Antarctic Peninsula during the second half of the 20th century. *Geophysical Research Letters* **32**, 1–5. DOI: http://dx.doi.org/10.1029/2005GL024042.

Meredith, M, Sommerkorn, M, Cassotta, S, Derksen, C, Ekaykin, A, Hollowed, A, Kofinas, G, Mackintosh, A, Melbourne-Thomas, J, Muelbert, MMC, Ottersen, G, Pritchard, H, Schuur, EAG. 2019. Polar regions, in Anisimov, O, Flato, G, Xiao, C, eds., *The ocean and cryosphere in a changing climate: Summary for policymakers.* Intergovernmental Panel on Climate Change: 3-1-3-173. Available at https://www.ipcc.ch/srocc/home.

Michel, C, Legendre, L, Demers, S, Therriault, J-C. 1988. Photoadaptation of sea-ice microalgae in springtime: Photosynthesis and carboxylating enzymes. *Marine Ecology Progress Series* **50**: 177–185.

Michel, C, Legendre, L, Therriault, J-C, Demers, S, Vandevelde, T. 1993. Springtime coupling between ice algal and phytoplankton assemblages in southeastern Hudson Bay, Canadian Arctic. *Polar Biology* **13**: 441–449.

Miller, L, Fripiat, F, Else, BGT, Bowman, JS, Brown, KA, Collins, E, Ewert, M, Fransson, A, Gosselin, M, Lannuzel, D, Meiners, KM, Michel, C, Nishioka, J, Nomura, D, Papadimitriou, S, Russell, LM, Sørensen, LL, Thomas, DN, Tison, J-L, van Leeuwe, MA, Vancoppenolle, M, Wolff, EW, Zhou, J. 2015. Methods for biogeochemical studies of sea ice: The state of the art, caveats, and recommendations. *Elementa Science of the Anthropocene* **3**: 000038. DOI: http://dx.doi.org/10.12952/journal.elementa.000038.

Mundy, CJ, Gosselin, M, Ehn, JK, Belzille, C, Poulin, M, Alou, E, Roy, S, Hop, H, Lessard, S, Papakyriakou, TN, Barber, DG, Stewart, J. 2011. Characteristics of two distinct high-light acclimated algal communities during advanced stages of sea ice melt. *Polar Biology* **34**: 1869–1886.

Olenina, I., Hajdu, S, Edler, L, Andersson, A, Wasmund, N, Busch, S, Göbel, J, Gromisz, S, Huseby, S, Huttunen, M, Jaanus, A, Kokkonen, P, Ledaine, I, Niemkiewicz, E. 2006. Biovolumes and size-classes of phytoplankton in the Baltic Sea. *HELCOM Baltic Sea Environment Proceedings* **106**, 144.

Palmisano, AC, Beeler Soohoo, J, Sullivan, CW. 1987. Effects of four environmental variables on photosynthesis-irradiance relationships in Antarctic sea-ice microalgae. *Marine Biology* **94**: 299–306.

Perrin, RA, Lu, P, Marchant, HJ. 1987. Seasonal variation in marine phytoplankton and ice algae at a shallow Antarctic coastal site. *Hydrobiologia* **146**: 33–46.

Platt, T, Gallegos, CL, Harrison, WG. 1980. Photoinhibition of photosynthesis in natural assemblages of marine phytoplankton. *Journal of Marine Research* **38**: 687–701.

Ratkova, TN, Wassmann, P. 2005. Sea ice algae in the White and Barents seas: Composition and origin. *Polar Research* **24**: 95–110.

Riaux-Gobin, C, Dieckmann, GS, Poulin, M, Neveux, J, Labrune, C, Vetion, G. 2013. Environmental conditions, particle flux and sympagic microalgal succession in spring before the sea-ice break-up in Adelie Land, East Antarctica. *Polar Research* **32**: 1. DOI: http://dx.doi.org/10.3402/polar.v32i0.19675.

Riebesell, U, Schloss, I, Smetacek, V. 1991. Aggregation of algae released from melting sea ice: Implications for seeding and sedimentation. *Polar Biology* **11**: 239–248.

Riedel, A, Michel, C, Gosselin, M, LeBlanc, B. 2008. Winter-spring dynamics in sea-ice carbon cycling in the coastal Arctic Ocean. *Journal of Marine Systems* **74**: 918–932.

Roach, LA, Dörr, J, Holmes, CR, Massonnet, F, Blockley, EW, Notz, D, Rackow, T, Raphael, MN, O'Farrell, SP, Bailey, DA, Bitz, CM. 2020. Antarctic sea-ice area in CMIP6. *Geophysical Research Letters* **47**(9). DOI: http://dx.doi.org/10.1029/2019GL086729.

Rozanska, M, Gosselin, M, Poulin, M, Wiktor, JM, Michel, C. 2009. Influence of environmental factors on the development of bottom ice protist communities during the winter–spring transition. *Marine Ecology Progress Series* **386**: 43–59.

Rozema, PD, Venables, HJ, Van de Poll, WH, Clarke, A, Meredith, MP, Buma, AGJ. 2017. Interannual variability in phytoplankton biomass and species composition in northern Marguerite Bay (West Antarctic Peninsula) is governed by both winter sea ice cover and summer stratification. *Limnology and Oceanography* **62**: 235–252. DOI: http://dx.doi.org/10.1002/lno.10391.

Saggiomo, M, Poulin, M, Mangoni, O, Lazzara, L, De Stefano, M, Sarno, D, Zigone, A. 2017. Spring-time dynamics of diatom communities in landfast and underlying platelet ice in Terra Nova Bay, Ross Sea, Antarctica. *Journal of Marine Systems* **166**: 26–36. DOI: http://dx.doi.org/10.1016/j.jmarsys.2016.06.007.

Scharek, R, Smetacek, V, Fahrbach, E, Gordon, LI, Rohardt, G, Moore, S. 1994. The transition from winter to early spring in the eastern Weddell Sea, Antarctica: Plankton biomass and composition in

relation to hydrography and nutrients. *Deep-Sea Research I* **41**: 1231–1250.

Selz, V, Laney, S, Arnsten, AE, Lewis, K, Lowry, KE, Joy-Warren, HL, Mills, MM, Van Dijken, GJ, Arrigo, KR. 2018a. Ice algal communities in the Chukchi and Beaufort Seas in spring and early summer: Composition, distribution, and coupling with phytoplankton assemblages. *Limnology and Oceanography* **63**: 1109–1133.

Selz, V, Lowry, K, Lewis, K, Van de Poll, W, Joy-Warren, H, Nimel, S, Tong, A, Arrigo, K. 2018b. Distribution of *Phaeocystis antarctica*-dominated sea ice algal communities and their potential to seed phytoplankton across the west Antarctic Peninsula in spring. *Marine Ecology Progress Series* **586**: 91–112.

Smith, WO, Nelson, DM. 1990. Phytoplankton growth and new production in the Weddell Sea marginal ice zone in austral spring and autumn. *Limnology and Oceanography* **35**(4): 809–821.

Søreide, JE, Leu, E, Berge, J, Graeve, M, Falk-Petersen, S. 2010. Timing in blooms, algal food quality and *Calanus glacialis* reproduction and growth in a changing Arctic. *Global Change Biology* **16**(11): 3154–3163. DOI: http://dx.doi.org/10.1111/j.1365-2486.2010.02175.x.

Stammerjohn, SE, Martinson, DG, Smith, RC, Yuan, X, Rind, D. 2008. Trends in Antarctic annual sea ice retreat and advance and their relation to El Niño–Southern Oscillation and Southern Annular Mode variability. *Journal of Geophysical Research* **113**, 1–20. DOI: http://dx.doi.org/10.1029/2007JC004269.

Stefels, J, Dacey, JWH, Elzenga, JTM. 2009. In vivo DMSP-biosynthesis measurements using stable-isotope incorporation and proton-transfer-reaction mass spectrometry (PTR-MS). *Limnology and Oceanography-Methods* **7**: 595–611.

Stefels, J, Steinke, M, Turner, S, Malin, G, Belviso, S. 2007. Environmental constraints on the production and removal of the climatically active gas dimethyl-sulphide (DMS) and implications for ecosystem modelling. *Biogeochemistry* **83**:245–275.

Stefels, J, van Leeuwe, MA, Jones, EJ, Meredith, MP, Venables, HJ, Webb, AL, Henley, SF. 2018. Impact of sea-ice melt on DMS(P) inventories in surface waters of Marguerite Bay, West Antarctic Peninsula. *Philosophical Transactions of the Royal Society A* **376**: 20170169.

Stoecker, DK, Gustafson, DE, Black, MMD, Baier, CT. 1998. Population dynamics of microalgae in the upper land-fast sea ice at a snow-free location. *Journal of Phycology* **34**: 60–69.

Szymanski, A, Gradinger, R. 2016. The diversity, abundance and fate of ice algae and phytoplankton in the Bering Sea. *Polar Biology* **39**: 309–325.

Tedesco, L, Vichi, M, Thomas, DN. 2012. Process studies on the ecological coupling between sea ice algae and phytoplankton. *Ecological Modelling* **226**: 120–138.

Thomas, DN ed. 2017. *Sea ice*, 3rd ed. Oxford, UK: Wiley-Blackwell: 652.

Turner, J, Lu, H, White, I, King, JC, Phillips, T, Hosking, JS, Bracegirdle, TJ, Marshall, GJ, Mulvaney, R, Deb, P. 2016. Absence of 21st century warming on Antarctic Peninsula consistent with natural variability. *Nature* **535**: 411–415.

Utermohl, H. 1958. Zur Vervollkommung der quatitative-ven Phytoplankton-Methodik. *Mitteilungen der Internationalen Verhandlung der Limnologie* **9**: 1–38.

Van Heukelem, L, Thomas, CS. 2001. Computer-assisted high-performance liquid chromatography method development with applications to the isolation and analysis of phytoplankton pigments. *Journal of Chromatography A* **910**: 31–49. DOI: http://dx.doi.org/10.1016/S0378-4347(00)00603-4.

Van Leeuwe, MA, Tedesco, L, Arrigo, KR, Assmy, P, Campbell, K, Meiners, KM, Rintala, J-M, Selz, V, Thomas, DN, Stefels, J. 2018. Microalgal community structure and primary production in Arctic and Antarctic sea ice: A synthesis. *Elementa Science of the Anthropocene* **6**: 4. DOI: http://dx.doi.org/10.1525/elementa.267.

Van Leeuwe, MA, Villerius, LA, Roggeveld, J, Visser, RJW, Stefels, J. 2006. An optimized method for automated analysis of algal pigments by HPLC. *Marine Chemistry* **102**: 267–275.

Van Leeuwe, MA, Webb, AL, Venables, H, Visser, RJW, Meredith, MP, Elzenga, JTM, Stefels, J. 2020. Annual patterns in phytoplankton phenology in Antarctic coastal waters explained by environmental drivers. *Limnology and Oceanography* **65**: 1651–1668. DOI: http://dx.doi.org/10.1002/lno.11477.

Zhang, R, Zheng, M, Chen, M, Ma, Q, Cao, J, Qiu, Y. 2014. An isotopic perspective on the correlation of surface ocean carbon dynamics and sea ice melting in Prydz Bay (Antarctica). *Deep-Sea Research I* **83**: 24–33.